

On Manipulator Posture Planning for Large Force Tasks

Evangelos Papadopoulos, Yves Gonthier

Department of Mechanical Engineering & Centre for Intelligent Machines
McGill University
Montreal, PQ, Canada H3A 2A7

Abstract

In this paper, we study the problem of large force/torque application using robotic systems with limited force/torque actuators. For such systems, the available workspace may be smaller than its reachable workspace. It is shown that redundancy increases the force capability and workspace of a robotic system. To plan redundant manipulator postures during force tasks, a new method based on a min-max optimization scheme is used. Unlike other norm-based methods, the proposed one guarantees that no actuator capabilities are exceeded, and that the required force/torque of the most loaded actuator is minimized. Examples that demonstrate the validity and usefulness of the proposed method are included.

1 Introduction

Humans display an extraordinary ability in developing and applying large forces to their environment, compared to their muscle force and torque capabilities. During a task requiring application of large forces, body posture may change adapting to task needs, and redundancy is utilized efficiently. On the other hand, robotic manipulators exhibit limited force/torque capabilities, even in static or quasi-static tasks. This issue becomes very important in mobile applications of robotic systems, where typically development of large forces is expected. In these applications, the position of a mobile system's base can be relocated with respect to a task, adding redundancy to the system. In cases where repetitious tasks are being planned, the robot can be positioned initially such that its posture is optimal for the given force task. In space, highly redundant systems such as the Special Purpose Dexterous Manipulators (SPDM) mounted on the Space Station Remote Manipulator System (SSRMS), see Fig. 1, are being built to operate in a gravity-less environment. Efficient application of forces in space becomes very important given the fact that actuators are typically small due to weight restrictions, and to the lack of the need to support a system's own weight.

Actuator limitations have been considered in studies of time optimal motion planning, and in resolving manipulator redundancy in motion control [1,2]. The force distribution problem in multi-limb systems has been studied using linear programming techniques, in conjunction to energy and load balancing performance indexes [3]. The necessary and sufficient conditions for applying a force to the envi-

ronment were presented in [4]. Posture control in motion or force tasks has been considered using velocity and force ellipsoids, and a task compatibility measure [5]. The direction and magnitude of maximum force/torque that can be applied at some given end-effector location has been studied to provide a basis for the task planning for force control of multiple cooperating robot arms [6]. A configuration-space based Force Workspace approach, originally proposed in [7], was used to plan motions of multi-limb systems without violating actuation and joint limits, or frictional constraints [7]. Redundancy resolution criteria were introduced based on desired motion or force task requirements [8].

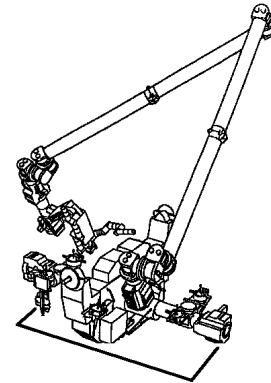


Fig. 1. The SPDM on the SSRMS

In this paper, we study the problem of large force/torque application using robotic systems with limited force/torque actuators. For a given desired end-effector force/torque, there exists a workspace with the property that if the end-effector is in it, then the desired force/torque can be applied without violating actuator constraints. Such a 'force workspace' is larger for redundant systems than for non-redundant systems with the same reachable workspace. To plan force tasks for redundant manipulators, a new method based on a min-max approach is used. For a given force task, the optimal manipulator posture is computed by first finding the maximum required normalized torque curve as a function of a redundancy parameter, and then by choosing this parameter such that the normalized torque at some posture is minimized. It is shown by examples how this method can be applied in planning force tasks. Finally this new method is compared with a widely used method based on

minimizing the sum of weighted squared forces/torques. It is shown that such method does not guarantee that actuator limits are not exceeded. In contrast, the proposed method guarantees that all joint torques will not exceed their limits. In addition, the torque level of the joint required to apply the largest normalized torque will ‘suffer’ the least possible, resulting in effective actuator use, and maximization of a robotic system’s force capabilities.

2 Force workspace

In this paper we focus on tasks which require the application of large forces or torques on the environment. For example, such tasks include holding or lifting large payloads, pushing heavy containers in warehouse operations, or removing of an Orbital Removable Unit (ORU) during some contingency operation in space. In such cases, inertial forces are relatively small or non-existent, and therefore such tasks can be considered as quasi-static or even static. Then, the equivalent torques/forces $\boldsymbol{\tau}$ required to apply a force/torque $\mathbf{F} = [\mathbf{f}^T, \mathbf{n}^T]^T$, where \mathbf{f} and \mathbf{n} are the force and moment applied by the end-effector to the environment, are given by

$$\boldsymbol{\tau} = \mathbf{J}(\mathbf{q})^T \mathbf{F} \quad (1)$$

where $\mathbf{J}(\mathbf{q})$ is the Jacobian of the manipulator [9]. We assume here that the manipulator structure is such that the force \mathbf{F} can be applied in any desired direction. However, since actuators are not ideal sources of force or torque, the forces/torques $\boldsymbol{\tau}$ are subject to constraints such as torque speed characteristics. In static or quasi-static cases, these result in maximum actuator force/torque limits given by

$$|\boldsymbol{\tau}| \leq \boldsymbol{\tau}_{\max} \quad (2)$$

For quasi-static tasks, $\boldsymbol{\tau}_{\max}$ is a function of the configuration \mathbf{q} . As the magnitude of the applied force \mathbf{F} is increased, it is expected that one or more actuators will saturate, i.e. they won’t be able to provide the necessary force/torque as required by the equivalent torques given by Eq. (1). If the magnitude of the force is further increased, then either the manipulator will have to change posture, move its base closer to the point of application, or fail in its task, sometimes with disastrous consequences.

It is interesting to examine what are the possible configurations (postures) at which the end-effector can apply a force with given magnitude and direction. This problem can be solved analytically in simple cases, but in general requires sophisticated search techniques. Such searching can be minimized by noting that at the boundaries of the region at which end-effector can still apply the given force, one or more actuators will saturate, i.e. $|\tau_i| = \tau_{i,\max}$. To demonstrate this notion, a simple two-link manipulator with equal links is employed. The link lengths are $l_1 = 1m, l_2 = .9m$, and the torque limits $\tau_{1,\max} = 10Nm, \tau_{2,\max} = 6Nm$. As depicted in Figure 2, when the force is very small, the end-effector can apply a force F along the x axis at any point in its reachable workspace. However, when the force magnitude increases to $12Nm$, the available ‘force workspace’ is reduced significantly.

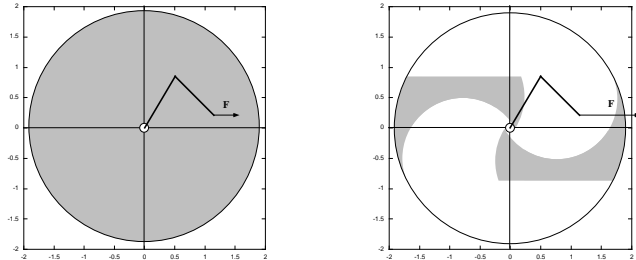


Fig.2 Workspace regions where force F can be applied. (a) Small F , (b) large F .

As shown in Fig. 2, the force workspace is delimited by two straight lines parallel to the force, at a distance $|\tau_{1,\max}|/|F|$ from the base of the manipulator. The workspace boundaries associated with the second joint saturation are obtained analytically by setting the second joint torque to its maximum value, and then solving for the possible end effector positions in Eq (1). For a two-link planar manipulator, the boundaries are four circles of radius l_1 centered at a distance l_2 from the base at the angle $q_1 = \pm [q_F - \arcsin(\tau_{2,\max}/l_2 F)]$ where q_F is the direction of the force F . For simplicity, the second joint is restricted to positive angles.

For planar manipulators, changing the force direction results in a simple rotation of the force workspace. For example, if the desired force F is rotated in the positive direction by 40° , then the shaded area in Fig. 2(b) will also rotate by the same angle, and this is where the manipulator will be able to apply the desired force.

Note that computing this workspace allows one to plan force tasks. A task is feasible if the end-effector belongs in the force workspace. If this is not the case, then either the base of the manipulator must relocate, or the task must be moved with respect to the base of the manipulator. The first case applies to mobile systems, whereas the second becomes important in repetitive operations. If any of these possibilities does not apply, the particular force task becomes non feasible.

We next focus on the effect of redundancy on the force workspace of a system. To this end, we compare two manipulators with the same reachable workspace boundary, and the same actuators. Their parameters are given in Table I. For both, the force task is to apply a force $F = 10.25 N$ at 0° . The force workspaces are obtained in each case. Fig 3(a) shows that two link manipulator is not capable of applying this force at the configuration shown, while the redundant manipulator, can successfully accomplish the same task, see Fig. 3(b). Physically, this is due to the fact that the joints of the redundant system can be positioned such that the moment arms are minimized.

Table I. Manipulator parameters

	l_1 (m)	l_2 (m)	l_3 (m)	$\tau_{1,\max}$ (Nm)	$\tau_{2,\max}$ (Nm)	$\tau_{3,\max}$ (Nm)
1	2.0	1.0	n/a	10.0	10.0	n/a
2	1.0	1.0	1.0	10.0	10.0	10.0

Obtaining the force workspace for a redundant manipulator requires that all possible configurations be examined before deciding if a particular end effector position is part of the workspace. This is done by expressing actuator torques/forces as functions of the redundant joint variables, and choosing values for these variables such that no joint actuator becomes saturated.

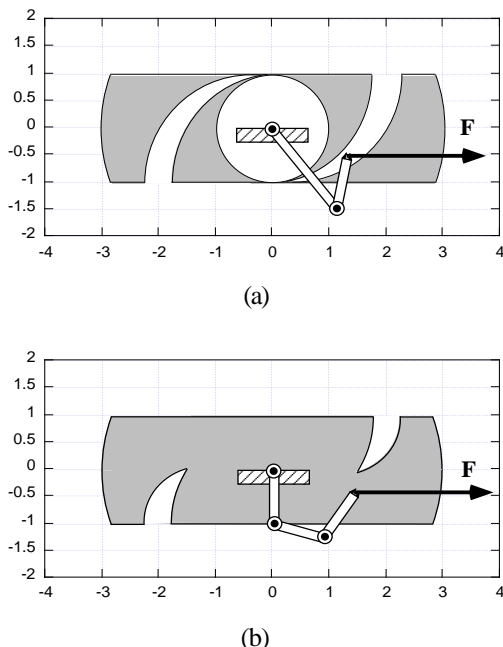


Fig. 3. Comparison of the force workspace for a non-redundant and a redundant manipulator with the same reachable workspace boundary.

3 Configuration planning for redundant manipulators

3.1 Optimal configurations during a force / torque task

A redundant manipulator has more degrees of freedom than the task requires. This allows one to choose additional conditions to be met. Typical such conditions include energy minimization, or manipulability maximization. A comprehensive review of related criteria can be found in [8]. To apply these criteria, some manipulator performance index is defined first, and then optimized to result in planning configurations and trajectories. However, a problem that arises is that these criteria affect the manipulator in an overall manner; i.e. they do not consider individual joint limitations. For example, optimizing the mechanical advantage in a manipulator, does *not* guarantee that individual joint actuator limits will not be exceeded. To avoid these problems, it is essential to determine first what is the workspace range where a manipulator can apply a given force, if any, and then consider criteria to be optimized within that range.

To demonstrate this concept, consider a three link planar manipulator, as shown in Fig. 3(b). Its joint actuators are subject to torque limits as specified by Eq. (2). Since these

limits are typically not the same, the torque at each joint is normalized with respect to its maximum absolute value. Therefore, it is required that all joint normalized force/torques do not exceed 1 in absolute value. Hence,

$$\left| \frac{\tau_i}{\tau_{i,\max}} \right| \leq 1 \quad (3)$$

Note that due to Eq. (1), the value of the ratio given by Eq. (3) is a function of the configuration \mathbf{q} of the manipulator. Using Eq. (3), and assuming some configuration \mathbf{q} , we can determine how much a particular joint actuator is loaded, and in addition, by computing this ratio for all joints, which actuator is loaded the most. The closer the normalized torque for some joint's actuator is to 1, the worse it is for this actuator.

For some given end-effector location, the normalized torques can be plotted as a function of the redundant variables, in this case as a function of q_1 . If in this plot there are ranges of q_1 for which Eq. (3) is satisfied, then the end-effector location lies in the force workspace, i.e. the end-effector force \mathbf{F} can be applied at this location. For example, Fig. 4 shows such a plot of normalized torques that corresponds to some end-effector location. Since for the ranges shown, all normalized torques are below 1, the desired force can be applied at the corresponding end-effector location. Since a range of angles q_1 is available, then a corresponding range of manipulator postures \mathbf{q} is also available.

In general, the range from which q_1 can be chosen is limited due to geometric considerations, or joint limits. For example, as shown in Fig. 4, no values between 0.92 and 3.15 rad are acceptable due to geometric limitations. When torque limitations are taken into account, the maximum normalized torque plot indicates two feasible ranges from which q_1 can be chosen, see Fig. 4. In these two regions, the maximum normalized torque is below or equal to 1. To optimize some given general criteria like power, would require optimization of the posture within these ranges.

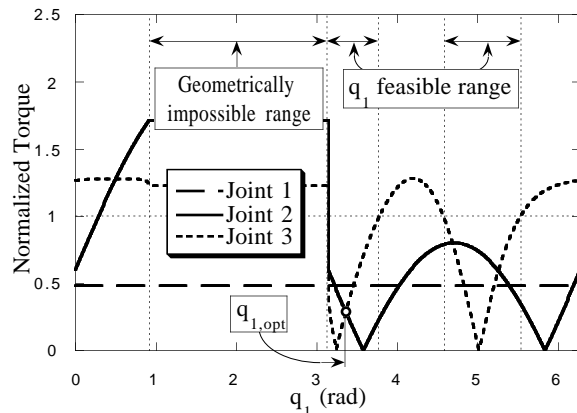


Fig. 4. Typical normalized torque variation as a function of the first joint angle, q_1 .

The next question we address is what the optimization criterion should be to guarantee that the force can be applied

without violating actuator limitations. To answer this question, we first define the optimal configuration as the one at which all actuators ‘suffer’ the least, i.e., the normalized torques are all as far as possible from 1. Mathematically, this criterion can be set as a min-max problem defined as follows: choose the optimal configuration \mathbf{q} such that it satisfies

$$U = \min_{\mathbf{q}_r} \max_i \left| \frac{\tau_i(\mathbf{q}_r)}{\tau_{i,\max}} \right| \quad (4)$$

where \mathbf{q}_r is the set of the redundant joint variables. To apply this criterion, one needs to find the maximum of the normalized torques as a function of \mathbf{q}_r and then find its minimum. This operation guarantees that all joints will have a load less or equal to U . In the case of a three link manipulator, if we choose as a redundant joint variable the first joint angle, q_1 , then the optimal q_1 is determined by

$$U = \min_{q_1} \max_{i=1,2,3} \left| \frac{\tau_i(q_1)}{\tau_{i,\max}} \right| \quad (5)$$

The other two joint angles can be found using standard inverse kinematic equations.

Applying the min-max criterion on the plot in Fig. 4 yields as the optimal angle $q_{1,\text{opt}} = 3.4$ rad. It is readily seen that this solution occurs where the normalized torques of joints 2 and 3 are equal. This makes physical sense. First, the first joint actuator has no incidence on the optimal configuration. This is because, whatever the configuration the manipulator adopts for a given end effector position, the moment arm with respect to joint 1 is the same. Basically, this joint can always support the torque, until the moment arm becomes greater than $|\tau_{1,\max}|/|F|$. However, for joints 2 and 3, the normalized torque is a function of the configuration, and it is natural that the best configuration will occur when these two joint “share” the load equally, taking into account their relative actuator limits. Looking at Fig. 4, we see that there are four points where the normalized torques of joints 2 and 3 are equal. (There are eight points if q_3 is allowed to be negative, but for simplicity, it has been assumed positive). These points can be found by using root finding algorithms like Newton’s method. Numerical difficulties are encountered at the geometric limits and singular configurations, especially when links are of equal lengths. These can be overcome using a small step size. Although only one such point (root) corresponds to the actual minimum, finding all the roots is useful for the next step: planning the configuration of the manipulator as it performs a task.

3.2 Force Task Planning. When a manipulator performs a task, such as pushing a heavy container, or removing an ORU, it must apply a force/torque along a path, S , parameterized by some variable s . Here again, we require that the actuator limits at the joints must not be exceeded. We can thus perform the same analysis as was done above to determine the range of possible q_1 and so forth. However, this can be long and tedious. Instead, we use an algorithm that tracks the angles q_1 at which two

normalized torques are equal. Since these are found using a root solver, we refer to them as the ‘roots’.

Note that since the motion of the end effector is continuous, the normalized torque variation graph, and the roots change gradually with s . Therefore, a new root can be found with a root solver using the previous one as a rough initial estimate. With a reasonable step size, fast convergence is achieved and the root can be ‘followed’ as a function of the path parameter, s . For example, Fig. 5 shows the evolution of angles q_1 at which two normalized torques have equal values, whereas Fig. 6 shows the corresponding normalized torque. The optimal configuration $q_{1,\text{opt}}(s)$ will consist of segments that belong to the curves shown in Fig. 5.

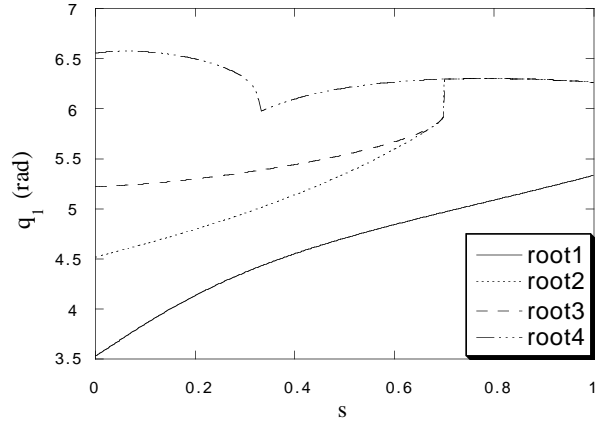


Fig. 5. Roots q_1 along a path S .

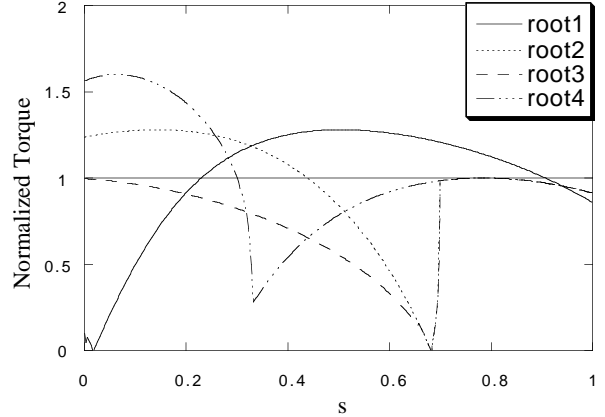


Fig. 6. Normalized torque values that correspond to roots shown in Fig. 5.

Looking at the normalized torque that corresponds to roots 2 and 4 in Fig. 6, we see that although they start off well above 1, they eventually fall below. On the other hand, the normalized torque that corresponds to root 1 starts off well below 1, but increases rapidly above it. Also, both in Fig. 5 and Fig. 6, the curves that correspond to roots 2 and 3 converge around $s=0.7$. This is the case when two separate roots become a single double root, and then disappear. At the point where they disappear, the normalized torque curve for joint 2 and 3 barely touch, and then they

separate as s is increased. The root finder algorithm then jumps to the next closest root, # 4 as can be seen in Fig. 5.

Fig. 6 is useful because it can be used to decide which root should be chosen so that the normalized torques are equal or less than 1. Then Fig. 5 is used to find the corresponding optimal configuration by specifying the value of q_1 . At any point s along S , the minimum in Eq. (4) corresponds to the root with the lowest normalized torque value, i.e. we choose the lowest curve in Fig. 6. For the case depicted in Figs. 5 and 6, the algorithm follows root 1, then root 3, root 4, root 3 again, root 4 again and finally root 1 (notice root 1 falls below root 4 around $s=0.95$). When we switch from one root to another, the manipulator changes configuration. However, during this time, it may not be able to apply the force. This is analogous to when we try to move large objects around. Sometimes, we must stop pushing, reposition ourselves, and continue pushing again.

If switching configurations is time demanding, or undesirable, then it can be minimized by following suboptimal configurations, i.e. configurations for which the normalized torques are below 1, but not minimum. However, in some cases switching cannot be avoided. For example, for the case shown in Figs. 5 and 6, the number of switchings can be reduced to just one. The corresponding solution is to follow root 3 until $s=0.7$, then switch to root 4 until the end of the path.

4 Example

The planning method presented in Section III is next applied to a three link manipulator, whose parameters are given in Table II.

Table II. Manipulator parameters

l_1 (m)	l_2 (m)	l_3 (m)	$\tau_{1,\max}$ (Nm)	$\tau_{2,\max}$ (Nm)	$\tau_{3,\max}$ (Nm)
1.4	1.0	0.6	10.0	5.0	3.0

The force task consists of applying a force of 8 N at 0° along S - a straight line connecting points A and B with coordinates $(x_A, y_A) = (0.3, -0.6)m$ and $(x_B, y_B) = (2.3, -0.6)m$, i.e. a motion parallel to the x-axis. Figs. 5 and 6 show the evolution of the roots as the end effector moves along S . Figures 7, and 8 depict the optimal solution normalized torques and corresponding q_1 -configurations. Notice that the graphs are not continuous: discontinuities correspond to switching of configurations.

As discussed above, a suboptimal solution is also possible if the number of switchings is reduced to one, and occurs at $s=0.7$. The results are displayed in Figs. 9. Fig. 10 shows the actual configurations along the path S .

The proposed method is compared next to a frequently used method which resolves the redundancy by minimizing the sum of weighted actuator squared torques

$$q_1 \text{ satisfies } \min\{w_1\tau_1^2(q_1) + w_2\tau_2^2(q_1) + w_3\tau_3^2(q_1)\} \quad (6)$$

Weights are needed especially in the case where prismatic and rotary actuators are used so that the criterion is uniform

in terms of units. Note that the min-max method proposed here does not suffer from this limitation. Also note that the criterion given by Eq. (6) does not guarantee that during a force task no actuators will saturate. Instead, it guarantees that the ‘power’ required will be minimal.

To compare the performance resulting from the use of Eq. (6) with the results obtained using the min-max criterion, we use Eq. (6) with unit weights. In such case, the criterion (6) given above roughly minimizes total power consumption. The resulting normalized torques in this case are shown in Fig. 11, while the corresponding q_1 -s configurations are shown in Fig. 12.

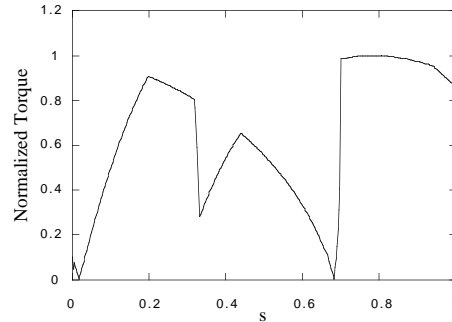


Fig. 7. Optimal normalized torque vs. path parameter s .

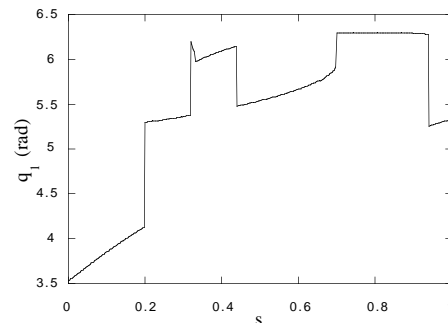


Fig. 8. Optimal q_1 -configuration vs. path parameter s .

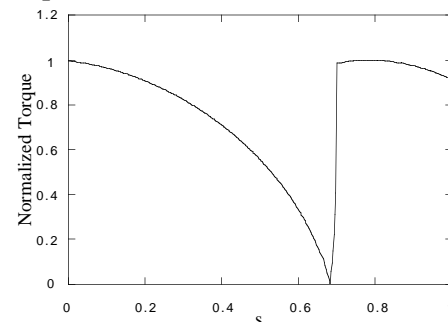


Fig. 9. Minimum switching normalized torque vs. Path

Fig. 11 shows that for a substantial part of the task, the required torque from actuator 3 exceeds the maximum available. Therefore, in the case where the desired end-effector force is large, this method will fail to yield feasible

posture histories. It should be noted that changing the weights in Eq. (6) will not alleviate this problem; increasing the weight on joint 3 will result in lower torques for it, but then other joints will saturate.

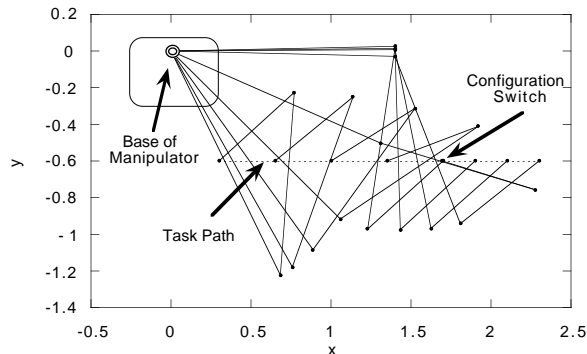


Fig. 10. Minimum switching configurations

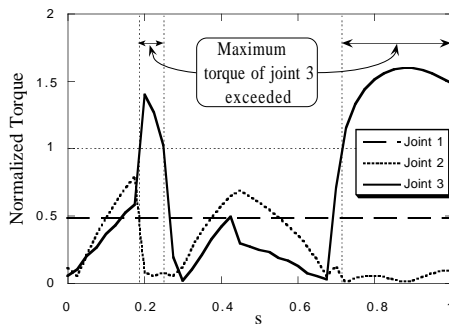


Fig. 11. Normalized torques using the criterion given by Eq. (6).

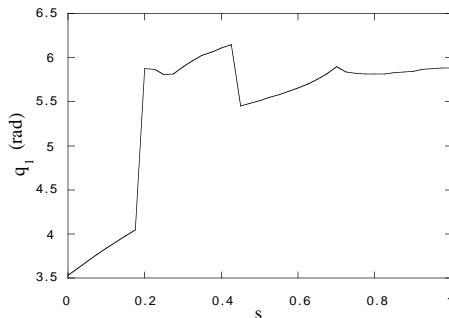


Fig. 12. Optimal angle q_1 using the criterion given by Eq. (6).

5 Conclusions

In this paper, we studied the problem of large force/torque application using robotic systems with limited force/torque actuators. For a given desired end-effector force/torque, there exists a workspace with the property that if the end-effector is in it, then the desired force/torque can be applied without violating actuator constraints. Such a ‘force workspace’ is larger for redundant systems than for non-redundant systems with the same reachable workspace. To plan force tasks of redundant manipulators, a new method based on a min-max

approach was proposed. For a given force task, the optimal manipulator posture is computed by first finding the maximum required normalized torque curve as a function of redundant joint variables, and then by choosing these variables such that the resulting normalized torque is minimized. It is shown by examples how this method can be applied in planning force tasks. Finally this new method is compared to a widely used method based on minimization of the sum of weighted squared forces/torques. It is shown that such methods do not guarantee that actuator limits will not be exceeded. In contrast, the min-max method guarantees that all joint torques will not exceed their maximum permitted values. In addition, the torque level of the joint required to apply the largest normalized torque will ‘suffer’ the least possible, resulting in effective use of a robotic system’s actuators.

Acknowledgments

The support of this work by the Fonds pour la Formation de Chercheurs et l’Aide a la Recherche (FCAR), and by the Natural Sciences and Engineering Council of Canada (NSERC) is gratefully acknowledged.

References

- [1] Bobrow, J. E., et al., “Time-Optimal Control of Robotic Manipulators along Specified Paths,” *Int. J. of Robotics Res.*, Vol. 4, No. 3, 1985, pp. 3-17.
- [2] Hollerbach, J. and Suh, K.C., “Redundancy Resolution of Manipulators through Torque Optimization,” *IEEE Tr. Robotics & Automation*, Vol. 3, No. 4, Aug. 1987, pp. 308-316.
- [3] Orin, D.E., and Oh, S.Y., “Control of Force Distribution in Robotic Mechanisms Containing Closed Kinematic Chains,” *ASME J. Dynamic Systems, Measurement, & Control*, Vol. 102, June 1981, pp. 134-140.
- [4] Nakamura, Y., “Force Applicability of Robotic Mechanisms,” *Proc. 26th Conference on Decision and Control*, Los Angeles, CA, Dec. 1987, pp. 570-575.
- [5] Chiu, S., “Control of Redundant Manipulators for Task Compatibility,” *Proc. IEEE Int. Conf. on Robotics & Automation*, Raleigh, NC, March 1987.
- [6] Li, Z., T.J. Tarn, and Bejczy, A., “Dynamic Workspace of Multiple Cooperating Robot Arms,” *IEEE Trans. Robotics & Automation*, Vol. 7, No. 5, Oct. 1991, pp. 589-596.
- [7] Madhani, A. and Dubowsky, S., “Motion Planning of Mobile Multi-Limb Robotic Systems Subject to Force and Friction Constraints,” *Proc. IEEE Int. Conf. on Robotics & Automation*, Nice, France, 1992, pp. 233-239.
- [8] Seraji, H., “Task-Based Configuration Control of Redundant Manipulators,” *J. of Robotic Systems*, 9(3), 1992, pp. 411-451.
- [9] Craig, J., *Introduction to Robotics, Mechanics and Control*, Addison Wesley, Reading, MA, 1989.